

Soft x-ray absorption spectroscopy study of Mo-rich $\text{SrMn}_{1-x}\text{Mo}_x\text{O}_3$ ($x \geq 0.5$)

J. H. Hwang, D. H. Kim, and J.-S. Kang*

Department of Physics, The Catholic University of Korea (CUK), Bucheon 420-743, Korea

S. Kolesnik, O. Chmaissem, J. Mais, and B. Dabrowski

Department of Physics, Northern Illinois University, DeKalb, Illinois 600115, USA

J. Baik and H. J. Shin

Pohang Accelerator Laboratory, POSTECH, Pohang 790-784, Korea

Jieun Lee, Bongjae Kim, and B. I. Min

Department of Physics, POSTECH, Pohang 790-784, Korea

(Received 16 August 2010; revised manuscript received 31 December 2010; published 24 February 2011)

Electronic structures of perovskite oxides of $\text{SrMn}_{1-x}\text{Mo}_x\text{O}_3$ in the Mo-rich regime ($x \geq 0.5$) have been investigated by employing soft x-ray absorption spectroscopy (XAS). Mn 2*p* XAS spectra of $\text{SrMn}_{1-x}\text{Mo}_x\text{O}_3$ indicate that the valence states of Mn ions are divalent and that they remain nearly unchanged for $x \geq 0.5$. On the other hand, the Mo 3*p* XAS spectra of $\text{SrMn}_{1-x}\text{Mo}_x\text{O}_3$ show some changes, suggesting that the valence states of Mo ions decrease with increasing x for $x \geq 0.5$. These conclusions are supported by the unoccupied Mn 3*d* and Mo 4*d* states, observed experimentally in the O 1*s* XAS spectra of $\text{SrMn}_{1-x}\text{Mo}_x\text{O}_3$.

DOI: [10.1103/PhysRevB.83.073103](https://doi.org/10.1103/PhysRevB.83.073103)

PACS number(s): 78.70.Dm, 74.25.Jb, 71.20.-b, 71.30.+h

$R_{1-x}A_x\text{MnO}_3$ -type manganese perovskite oxides (R , trivalent rare-earth ion; A , divalent Ca, Sr, Ba, etc.), having mixed-valent Mn ions, exhibit the colossal magnetoresistance (CMR) phenomena, the charge-ordered states near the half-filling ($x = 1/2$) with a concomitant first-order metal-insulator (M-I) transition, and the rich phase diagram.^{1,2} Likewise, doping of the Mn site with different transition-metal (TM) elements shows interesting phenomena, such as large room-temperature magnetoresistance (MR) and M-I transition in double perovskites.³ It was reported that a Mo substitution in LaMnO_3 induces ferromagnetism (FM), which originates from a double-exchange (DE) interaction between Mn^{3+} and Mn^{2+} ions.⁴ The advantage of Mo substitution for Mn is that a large variation in the Mn valence is possible due to the high valency of a Mo ion (Mo^{5+} or Mo^{6+}), while the structural disorder in the Mn lattice is relatively small.

SrMnO_3 is also a parent compound of the widely studied mixed-valent perovskite manganites, and it is a G -type antiferromagnetic (AFM) insulator ($T_N \sim 233$ K) with tetravalent Mn^{4+} ions.^{5,6} The ordered half-substitution in $\text{SrMn}_{1-x}\text{Mo}_x\text{O}_3$ corresponds to a double perovskite, $\text{Sr}_2\text{MnMoO}_6$, which is a monoclinically distorted AFM insulator ($T_N \sim 12$ K).⁷ For $\text{Sr}_2\text{MnMoO}_6$, the valence states of the Mn-Mo ions have been controversial between ($\text{Mn}^{2+}\text{-Mo}^{6+}$)⁷⁻⁹ and ($\text{Mn}^{3+}\text{-Mo}^{5+}$).¹⁰ Band structure calculations suggest that ($\text{Mn}^{2+}\text{-Mo}^{6+}$) is more likely.¹¹⁻¹³ The other end member SrMoO_3 in $\text{SrMn}_{1-x}\text{Mo}_x\text{O}_3$ is a paramagnetic metal.¹⁴ In particular, SrMoO_3 is known to have the lowest resistivity among all the oxides.¹⁵ In the Mo-rich regime, the M-I transition occurs in $\text{SrMo}_{1-y}\text{Mn}_y\text{O}_3$ for $y \geq 0.03$, accompanied by the change in the magnetic property from Pauli paramagnetism to Curie-Weiss paramagnetism for $y \geq 0.01$. The lattice constant increased with increasing Mn doping in $\text{SrMo}_{1-y}\text{Mn}_y\text{O}_3$, which suggested the existence of Mn^{2+} states, since the radius of a Mn^{2+} ion (0.67 Å) is similar to that of a Mo^{4+} ion (0.65 Å) while that of a Mn^{4+} ion (0.53 Å) is much smaller than that of a Mo^{4+} ion (0.65 Å).

In our previous study on the electronic structures of $\text{SrMn}_{1-x}\text{Mo}_x\text{O}_3$ in the low-concentration regime of the Mo substitution,¹⁶ we have found that the valence states of Mn ions decrease gradually from the high-spin (HS) tetravalent state (Mn^{4+} , $3d^3$) at $x = 0$ to the HS divalent state (Mn^{2+} , $3d^5$) at $x = 0.5$. The origin of the decreasing valence states of Mn ions with increasing x for $x \leq 0.5$ was due to the higher valence states of Mo ions that were close to being hexavalent (Mo^{6+}) for $x \leq 0.5$ in $\text{SrMn}_{1-x}\text{Mo}_x\text{O}_3$. Nevertheless, no work has been reported yet on the electronic structures of $\text{SrMn}_{1-x}\text{Mo}_x\text{O}_3$ for $x \geq 0.5$. Therefore it is important to determine the valence states of both Mn and Mo ions in $\text{SrMn}_{1-x}\text{Mo}_x\text{O}_3$ in the Mo-rich regime ($x \geq 0.5$).

In this work, we investigate the electronic structures of $\text{SrMn}_{1-x}\text{Mo}_x\text{O}_3$ in the Mo-rich regime ($x \geq 0.5$) by employing soft x-ray absorption spectroscopy (XAS), which is known to be a powerful experimental tool for studying the valence and spin states of TM ions in solids. This work provides the experimental evidence for the decreasing valence states of Mo ions in $\text{SrMn}_{1-x}\text{Mo}_x\text{O}_3$ for $x \geq 0.5$.

High-quality polycrystalline samples of $\text{SrMn}_{1-x}\text{Mo}_x\text{O}_3$ ($x \geq 0.5$) were synthesized by standard solid-state reaction methods. X-ray diffraction and neutron powder diffraction measurements showed that all the samples employed in this work have no impurity phase. The $\text{SrMn}_{1-x}\text{Mo}_x\text{O}_3$ samples for $0.5 \leq x \leq 0.75$ are monoclinically distorted double perovskites. Figure 1 shows the temperature-dependent resistivity $\rho(T)$ of $\text{SrMn}_{1-x}\text{Mo}_x\text{O}_3$ for $x \geq 0.5$. As x increases from $x = 0.5$, $\rho(T)$ decreases rapidly. This trend reflects the itinerant nature of Mo 4*d* states, which is consistent with the measured Mo 3*p* XAS (see Fig. 3).

XAS measurements were performed at the U7 beamline of the Pohang Light Source (PLS). The chamber pressure was better than 3×10^{-10} Torr. All the samples were cleaned *in situ* by repeated scrapings with a diamond file to remove the surface contamination. XAS spectra were obtained at room

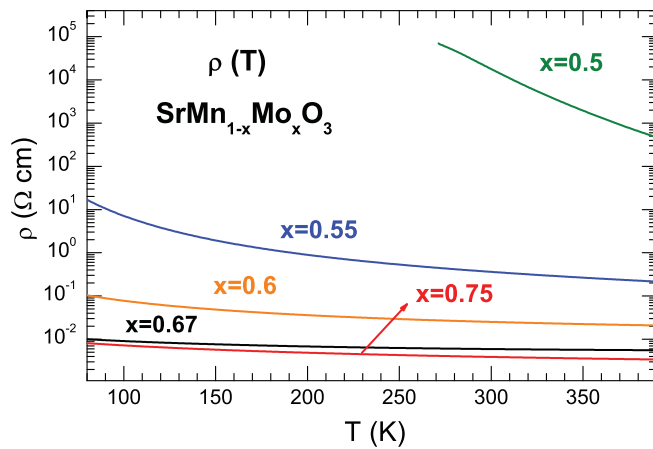


FIG. 1. (Color online) Temperature-dependent resistivity data for $\text{SrMn}_{1-x}\text{Mo}_x\text{O}_3$ ($x \geq 0.5$).

temperature by employing the total electron yield mode with a photon energy resolution of ~ 100 meV at $h\nu \approx 600$ eV. All the XAS spectra were normalized to the incident photon flux.

Figure 2 compares the measured Mn $2p$ XAS spectra of $\text{SrMn}_{1-x}\text{Mo}_x\text{O}_3$ ($x \geq 0.5$). All the spectra are split into L_3 ($2p_{3/2}$) and L_2 ($2p_{1/2}$) parts due to the $2p$ core-hole spin-orbit coupling. It is clearly shown that the Mn $2p$ XAS spectra remain essentially the same with increasing x for $x \geq 0.5$. TM $2p$ XAS is highly sensitive to its valence state by reflecting the $2p$ core-hole final-state multiplets due to the interaction between the $2p$ hole and the $3d$ electrons, where the number of $3d$ electrons plays an important role. Therefore the TM $2p$ XAS spectra of TM oxides represent the valence states of TM ions very well.

By comparing these Mn $2p$ XAS spectra to those of reference manganese oxides, such as MnO_2 (Mn^{4+}),¹⁷ Mn_2O_3 (Mn^{3+}),¹⁸ and MnO (Mn^{2+}),¹⁹ the valence states of Mn ions

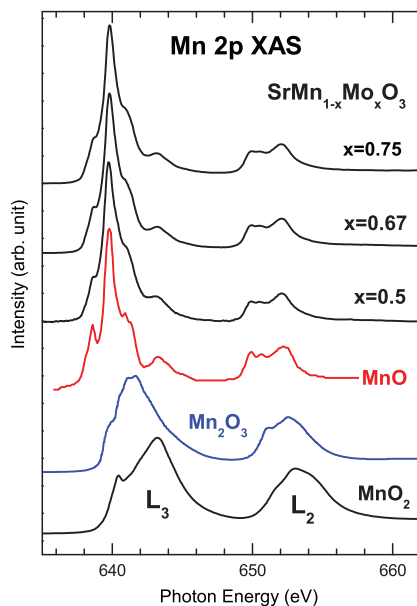


FIG. 2. (Color online) Comparison of the Mn $2p$ XAS spectra of $\text{SrMn}_{1-x}\text{Mo}_x\text{O}_3$ ($x \geq 0.5$) with those of MnO (Mn^{2+}), Mn_2O_3 (Mn^{3+}), and MnO_2 (Mn^{4+}).

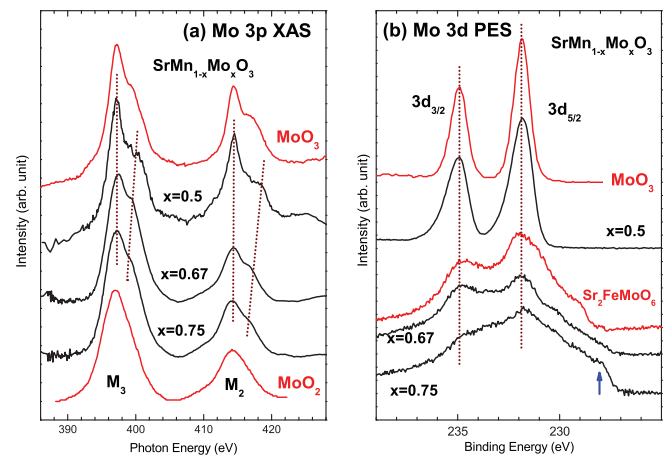


FIG. 3. (Color online) (a) Comparison of the Mo $3p$ XAS spectra of $\text{SrMn}_{1-x}\text{Mo}_x\text{O}_3$ ($x \geq 0.5$) with those of MoO_3 and MoO_2 . (b) Comparison of the Mo $3d$ core-level PES spectra of $\text{SrMn}_{1-x}\text{Mo}_x\text{O}_3$ ($x \geq 0.5$) with those of MoO_3 and $\text{Sr}_2\text{FeMoO}_6$.

in $\text{SrMn}_{1-x}\text{Mo}_x\text{O}_3$ can be identified. The Mn $2p$ XAS spectra of reference Mn oxides show that, as the nominal valence states of Mn ions increase from Mn^{2+} to Mn^{3+} and Mn^{4+} , the positions of the main peaks shift toward a high energy with the accompanying line shape change. This comparison provides evidence that the formal valence states (v) of Mn ions in $\text{SrMn}_{1-x}\text{Mo}_x\text{O}_3$ remain approximately $v \approx 2$ for $x \geq 0.5$. This finding makes a contrast to the case for $x \leq 0.5$ in $\text{SrMn}_{1-x}\text{Mo}_x\text{O}_3$, where the valence states of Mn ions decrease gradually from being tetravalent (Mn^{4+} , $3d^3$) at $x = 0$ to being divalent (Mn^{2+} , $3d^5$) at $x = 0.5$. Further, this finding implies that, as x increases from 0.5 in $\text{SrMn}_{1-x}\text{Mo}_x\text{O}_3$, the valence states of Mo ions should decrease from being hexavalent (Mo^{6+}) at $x = 0.5$.

Figure 3(a) compares the Mo $3p$ XAS spectra of $\text{SrMn}_{1-x}\text{Mo}_x\text{O}_3$ ($x \geq 0.5$), in comparison with those of reference Mo oxides, such as hexavalent MoO_3 (Mo^{6+} , $4d^0$) (top) and tetravalent MoO_2 (Mo^{4+} , $4d^2$)²⁰ (bottom). The peak positions and the linewidths of the Mo $3p$ XAS spectra of reference Mo oxides, having different nominal valence states, are very similar to each other. This is probably due to the rather delocalized nature of $4d$ TM electrons (see Fig. 1). The main differences between MoO_3 (Mo^{6+}) and MoO_2 (Mo^{4+}) are their line shapes: the Mo $3p$ XAS spectrum of hexavalent MoO_3 exhibits a double-peak structure clearly, while that of tetravalent MoO_2 exhibits a single, broad structure. The measured Mo $3p$ XAS spectrum for $x = 0.5$ is very similar to that of MoO_3 , showing a double-peak structure for both M_3 ($3p_{3/2}$) and M_2 ($3p_{1/2}$) parts. This finding supports the previous finding that Mo ions at $x = 0.5$ in $\text{SrMn}_{1-x}\text{Mo}_x\text{O}_3$ are hexavalent.¹⁶ With increasing x from $x \geq 0.5$, the line shape of the Mo $3p$ XAS spectrum becomes broad, and the line shape for $x = 0.75$ becomes very similar to that of MoO_2 , which has nominally tetravalent Mo^{4+} ions. It is not easy to tell how the peak positions change with x in $\text{SrMn}_{1-x}\text{Mo}_x\text{O}_3$ because the double peaks at $x = 0.5$ seem to merge with increasing x . Nevertheless, Fig. 3 shows that the valence states of Mo ions decrease from being hexavalent (Mo^{6+}) at $x = 0.5$ to the lower valence states at $x > 0.5$.

Figure 3(b) compares the Mo 3*d* core-level photoemission spectroscopy (PES) spectra of SrMn_{1-x}Mo_xO₃ for $x \geq 0.5$ to those of reference oxides of MoO₃ and Sr₂FeMoO₆, which are chosen as a formally hexavalent Mo⁶⁺ system and the Mo⁵⁺-Mo⁶⁺ mixed-valent system,²¹ respectively. The Mo 3*d* PES spectra of SrMn_{1-x}Mo_xO₃ were obtained at the U7 beamline at room temperature from the same samples from which the XAS data were obtained. The data for MoO₃ are taken from Ref. 22, while that for Sr₂FeMoO₆ is taken from Ref. 21. Note that the Mo 3*d* PES spectrum of SrMn_{1-x}Mo_xO₃ with $x = 0.5$ is very similar to that of MoO₃, indicating that the valence states of Mo ions are nearly hexavalent (Mo⁶⁺) at $x = 0.5$. In contrast, the Mo 3*d* PES spectra of SrMn_{1-x}Mo_xO₃ with $x = 0.67$ and $x = 0.75$ are much broader than that with $x = 0.5$ and they exhibit several peaks in contrast to the single-peak structure in MoO₃. The appearance of the extra features at the lower binding energies (BEs) is very similar to that of Sr₂FeMoO₆, which is known to be formally mixed-valent with the Mo⁵⁺-Mo⁶⁺ configuration and to have a metallic ground state.²¹ Further, the Mo 3*d* PES spectra for $x > 0.5$ reveal the extra emission at BEs (marked with an arrow) lower than those in Sr₂FeMoO₆. These findings suggest that, for $x > 0.5$, the valence states of Mo ions are lower than those of Mo⁶⁺ ions and also lower than those in Sr₂FeMoO₆. In other words, for $x > 0.5$, Mo ions are mixed-valent either with the Mo⁴⁺-Mo⁶⁺ configuration or with the Mo⁴⁺-Mo⁵⁺-Mo⁶⁺ configuration.

The top of Fig. 4 shows the O 1*s* XAS spectra of SrMn_{1-x}Mo_xO₃ for $x \geq 0.5$. The O 1*s* XAS spectra of TM oxides represent the unoccupied TM 3*d* and *sp* states, as well as the other conduction-band states via the hybridization with the O 2*p* states.²³ The lowest-energy peaks in the O 1*s* spectra, which are marked as the bars in red and black, are identified as the unoccupied Mn 3*d* and Mo 4*d* states,²³ respectively. The broad peaks around $h\nu \sim 535$ eV are due to the unoccupied Sr 4*d* states,²³ and the peaks at ~ 540 – 545 eV are assigned to the unoccupied Mn 4*s*/4*p* and Mo 5*s*/5*p* states.

This figure reveals that, at $x = 0.5$, the unoccupied Mn 3*d* states lie closer to the Fermi level (E_F) than the unoccupied Mo 4*d* states. With increasing x from $x = 0.5$, the positions of the Mo 4*d* states shift down toward E_F . This trend can be explained by a simplified ionic model, shown in Fig. 4 (bottom) as a schematic energy diagram. Mn ions are divalent for $x \geq 0.5$, having the 3*d*⁵ ($t_{2g}^3 \uparrow e_g^2 \uparrow$) configuration (see Fig. 2). On the other hand, the valence states of Mo ions are hexavalent (Mo⁶⁺) at $x = 0.5$, with the configuration of 4*d*⁰ (t_{2g}^0), and they decrease to either Mo⁴⁺ or Mo⁵⁺ states with increasing x (see

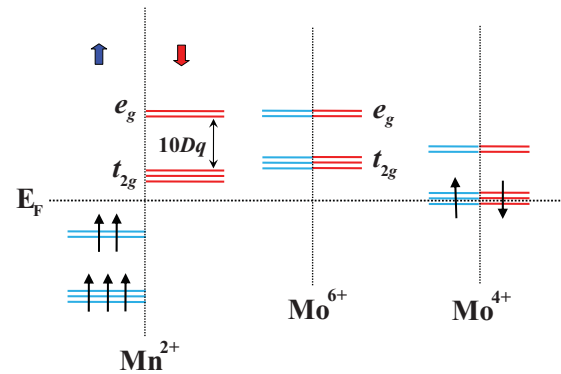
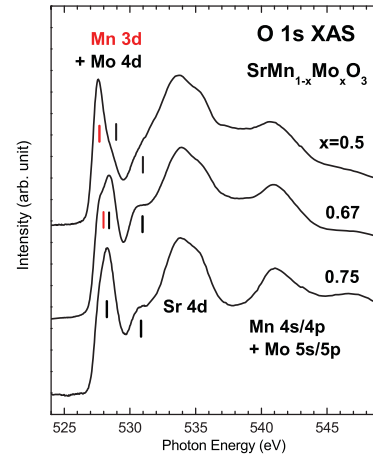


FIG. 4. (Color online) (Top) O 1*s* XAS spectra of SrMn_{1-x}Mo_xO₃ with $x = 0.5, 0.67,$ and 0.75 . Red and black bars are identified as the unoccupied Mn 3*d* and Mo 4*d* states, respectively. (Bottom) Schematic energy diagram for HS Mn²⁺ ($3d^5, t_{2g}^3 \uparrow e_g^2 \uparrow$), Mo⁶⁺ ($4d^0$), and Mo⁴⁺ ($4d^2, t_{2g}^2 \uparrow \downarrow$) ions, respectively.

Fig. 3). Note that Mn and Mo in SrMn_{1-x}Mo_xO₃ have the HS and low-spin states, respectively.²⁴ Hence the lowest-energy peaks in the O 1*s* XAS with $x = 0.5$ will correspond to the unoccupied Mn $t_{2g} \downarrow$ states, and the unoccupied Mo $t_{2g} \uparrow \downarrow$ states lie higher than the unoccupied Mn $t_{2g} \downarrow$ states. If Mo ions are tetravalent (Mo⁴⁺), having the $4d^2$ ($t_{2g}^2 \uparrow \downarrow$) configuration, then the partially filled Mo t_{2g} states for Mo⁴⁺ ions will be located closer to E_F than the vacant Mo t_{2g} states for Mo⁶⁺ ions. Therefore, as the valence state of a Mo ion decreases, the positions of the unoccupied Mo 4*d* states are expected to

TABLE I. Valence states of Mn and Mo in SrMn_{1-x}Mo_xO₃.

	$x = 0$	$0 < x < 0.5$	$x = 0.5$	$0.5 < x < 1$	$x = 1$
Mn	4+	$x\text{Mn} = 2+;$ $(1 - 2x)\text{Mn} = 4+$	2+	2+	
Average	4+	$(4 - 6x)/(1 - x)$	2+	2+	
Mo		6+	6+	$(1 - x)\text{Mo} = 6+;$ $(2x - 1)\text{Mo} = 4+$	4+
Average		6+	6+	$2(1 + x)/x$	4+

shift toward E_F due to the partial filling of the Mo t_{2g} states. This explains the observed trend in the O $1s$ XAS spectra reasonably well.²⁵

The previous¹⁶ and present findings for $\text{SrMn}_{1-x}\text{Mo}_x\text{O}_3$ suggest that, when a Mn^{4+} ion in SrMnO_3 is replaced by a Mo^{4+} ion, there occurs charge transfer from a Mo ion to a neighboring Mn ion, resulting in the $\text{Mo}^{6+}\text{-Mn}^{2+}$ configuration, as compared to the initial $\text{Mo}^{4+}\text{-Mn}^{4+}$ configuration. That is, the valence states of Mn and Mo in $\text{SrMn}_{1-x}\text{Mo}_x\text{O}_3$ are expected to vary with x as described in Table I in the ionic picture, even though the itinerant character is more appropriate to describe the Mo $4d$ electronic states in $\text{SrMn}_{1-x}\text{Mo}_x\text{O}_3$ for $x > 0.5$. Then the average valence state of Mn for $0 \leq x \leq 0.5$ is given by $(4 - 6x)/(1 - x)$, while that of Mo for $0.5 \leq x \leq 1$ is given by $2(1 + x)/x$.

In conclusion, we have studied the electronic structures of $\text{SrMn}_{1-x}\text{Mo}_x\text{O}_3$ ($x \geq 0.5$) by employing XAS. The measured

Mn $2p$ XAS spectra indicate that the valence states of Mn ions are nearly divalent and that they remain nearly unchanged for $x \geq 0.5$. On the other hand, the Mo $3p$ XAS and Mo $3d$ core-level PES spectra for $x \geq 0.5$ show the clear changes that imply the decreasing valence states of Mo ions from Mo^{6+} at $x = 0.5$ to the lower valence states (Mo^{4+} or Mo^{5+}) at $x > 0.5$. These conclusions are supported by the trends in the unoccupied Mn $3d$ and Mo $4d$ states in the O $1s$ XAS spectra, which occur due to the changes in their valence states.

This work was supported by the NRF under Contracts No. 2009-0064246 and No. 2009-0079947 and in part by the 2010 Research Fund of the CUK. The experiment at PLS was supported by POSTECH and MEST. Work at NIU was supported by the NSF (Grant No. DMR-0706610).

*kangjs@catholic.ac.kr

¹P. Schiffer, A. P. Ramirez, W. Bao, and S.-W. Cheong, *Phys. Rev. Lett.* **75**, 3336 (1995).

²Y. Tomioka, A. Asamitsu, Y. Moritomo, H. Kuwahara, and Y. Tokura, *Phys. Rev. Lett.* **74**, 5108 (1995).

³K.-I. Kobayashi, T. Kimura, H. Sawada, K. Terakura, and Y. Tokura, *Nature (London)* **395**, 677 (1998).

⁴W. J. Lu, Y. P. Sun, B. C. Zhao, X. B. Zhu, and W. H. Song, *Phys. Rev. B* **73**, 174425 (2006).

⁵K. Kikuchi, H. Chiba, M. Kikuchi, and Y. Syono, *J. Solid State Chem.* **146**, 1 (1999).

⁶O. Chmaissem, B. Dabrowski, S. Kolesnik, J. Mais, D. E. Brown, R. Kruk, P. Prior, B. Pyles, and J. D. Jorgensen, *Phys. Rev. B* **64**, 134412 (2001).

⁷M. Itoh, I. Ohta, and Y. Inaguma, *Mater. Sci. Eng. B* **41**, 55 (1996).

⁸A. Muñoz, J. A. Alonso, M. T. Casais, M. J. Martínez-Lope, and M. T. Fernández-Díaz, *J. Phys. Condens. Matter* **14**, 8817 (2002).

⁹J. H. Jung, S.-J. Oh, M. W. Kim, T. W. Noh, J.-Y. Kim, J.-H. Park, H.-J. Lin, C. T. Chen, and Y. Moritomo, *Phys. Rev. B* **66**, 104415 (2002).

¹⁰Y. Moritomo, Sh. Xu, A. Machida, T. Akimoto, E. Nishibori, M. Takata, and M. Sakata, *Phys. Rev. B* **61**, R7827 (2000).

¹¹H. Wu, *Phys. Rev. B* **64**, 125126 (2001).

¹²I. V. Solovyev, *J. Magn. Magn. Mater.* **268**, 194 (2004).

¹³Z. Yang and L. Ye, *J. Phys. Condens. Matter* **17**, 2035 (2005).

¹⁴S. B. Zhang, Y. P. Sun, B. C. Zhao, X. Luo, C. Y. Hao, X. B. Zhu, and W. H. Song, *J. Appl. Phys.* **102**, 103903 (2007).

¹⁵I. Nagai, N. Shirakawa, S. Ikeda, R. Iwasaki, H. Nishimura, and M. Kosaka, *Appl. Phys. Lett.* **87**, 024105 (2005).

¹⁶J. Lee, B. Kim, B. H. Kim, B. I. Min, S. Kolesnik, O. Chmaissem, J. Mais, B. Dabrowski, H. J. Shin, D. H. Kim, H. J. Lee, and J.-S. Kang, *Phys. Rev. B* **80**, 205112 (2009).

¹⁷Our data.

¹⁸P. Ghigna, A. Campana, A. Lascialfari, A. Caneschi, D. Gatteschi, A. Tagliaferri, and F. Borgatti, *Phys. Rev. B* **64**, 132413 (2001).

¹⁹C. Mitra, Z. Hu, P. Raychaudhuri, S. Wirth, S. I. Csiszar, H. H. Hsieh, H.-J. Lin, C. T. Chen, and L. H. Tjeng, *Phys. Rev. B* **67**, 092404 (2003).

²⁰R. S. Liu, T. S. Chan, S. Mylswamy, J. M. Chen, and J. P. Attfield, *Chin. J. Phys.* **43**, 751 (2005); R. S. Liu, Project report, NSC 93-2113-M-002-006, 1994.

²¹J. H. Kim, S. C. Wi, S. Yoon, B. J. Suh, J.-S. Kang, S. W. Han, K. H. Kim, A. Sekiyama, S. Kasai, S. Suga, C. G. Olson, B. J. Park, and B. W. Lee, *J. Korean Phys. Soc.* **43**, 416 (2003).

²²M. Sing, R. Neudert, H. von Lips, M. S. Golden, M. Knupfer, J. Fink, R. Claessen, J. Mücke, H. Schmitt, S. Hüfner, B. Lommel, W. Assmus, Ch. Jung, and C. Hellwig, *Phys. Rev. B* **60**, 8559 (1999).

²³J.-S. Kang, H. J. Lee, G. Kim, D. H. Kim, B. Dabrowski, S. Kolesnik, Hangil Lee, J.-Y. Kim, and B. I. Min, *Phys. Rev. B* **78**, 054434 (2008).

²⁴J.-S. Kang, H. J. Lee, D. H. Kim, S. Kolesnik, B. Dabrowski, K. Swierczek, J. Lee, B. Kim, and B. I. Min, *Phys. Rev. B* **80**, 045115 (2009).

²⁵More detailed understanding of the O $1s$ XAS requires the comparison of the O $1s$ XAS spectra with the calculated unoccupied partial densities of states (PDOSs) of $\text{SrMn}_{1-x}\text{Mo}_x\text{O}_3$ for the corresponding x value, where the effects of the Mn-O and Mo-O hybridization are included.